

RESULTS OF TESTING A CENTRIFUGAL BUBBLE SINGLET-OXYGEN GENERATOR

M. V. Zagidullin, V. D. Nikolaev,
M. I. Svistun, and N. A. Khvatov

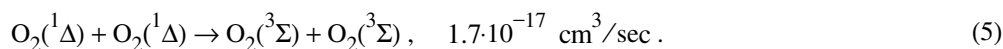
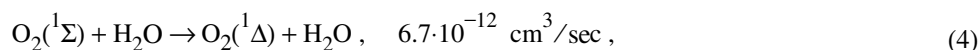
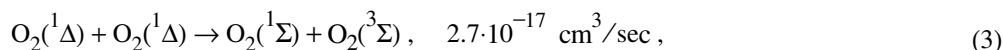
UDC 542.72:621.373.826.038.823

The results of parametric tests of a centrifugal bubble singlet-oxygen generator based on the reaction of chlorine with an alkaline hydrogen peroxide solution have been given. The utilization of chlorine grows with bubble-layer height, whereas the relative content of $O_2(^1\Delta)$ remains constant. Growth in centrifugal acceleration leads to a more efficient utilization of chlorine. A specific oxygen output of more than $1 \text{ mmole}\cdot\text{cm}^{-2}\cdot\text{sec}^{-1}$ from the bubble layer for a degree of chlorine utilization of $\sim 95\%$ and a singlet-oxygen yield of more than 50% has been attained. It has been shown that a centrifugal bubble singlet-oxygen generator is an efficient energy source for an oxygen-iodine laser.

The $^1\Delta$ state of oxygen is the first electronically excited oxygen state offset by 94.3 kJ/mole in energy from the ground state $^3\Sigma$ and having a radiation lifetime of more than 60 min. The singlet-oxygen $O_2(^1\Delta)$ is most efficiently formed in a singlet-oxygen generator (SOG) based on the reaction of chlorine with an alkaline hydrogen peroxide solution:



The initial concentration of HO_2^- ions is virtually equal to the concentration of the alkali, since the equilibrium of the reaction $\text{OH}^- + \text{H}_2\text{O}_2 \leftrightarrow \text{HO}_2^- + \text{H}_2\text{O}$ is strongly shifted to the right. For a rate constant of reaction (1) of $\sim 10^8$ liters/mole/sec and a concentration of the alkali of ~ 1 mole/liter, oxygen is formed at a distance of $\sim 10^{-7}$ cm from the surface of the alkaline hydrogen peroxide solution and the time of its diffusion yield from the liquid is $\sim 10^{-8}$ sec. Because of the small depth at which oxygen is formed and its low solubility in the alkaline hydrogen peroxide solution, the flux density of the oxygen released from the alkaline hydrogen peroxide solution is equal to the density of the adsorbed chlorine flux. Once $O_2(^1\Delta)$ has been released from the alkaline hydrogen peroxide solution, its loss is determined mainly by the decomposition in the series of reactions



Here $O_2(^1\Sigma)$ is the oxygen in a higher electronically excited state (157 kJ/mole). For example, at an initial $O_2(^1\Delta)$ pressure of 20 mm Hg, its content is halved over a period of ~ 25 msec. An SOG is a typical gas-liquid mass exchanger whose end product is the electronically excited oxygen $O_2(^1\Delta)$. Furthermore, at its output, there are the resid-

Samara Branch of the P. N. Lebedev Physical Institute, Russian Academy of Sciences, 221 Novosadovaya Str., Samara, 443011, Russia; email: marsel@fian.smr.ru. Translated from *Inzhenerno-Fizicheskii Zhurnal*, Vol. 80, No. 3, pp. 121–128, May–June, 2007. Original article submitted April 12, 2006.

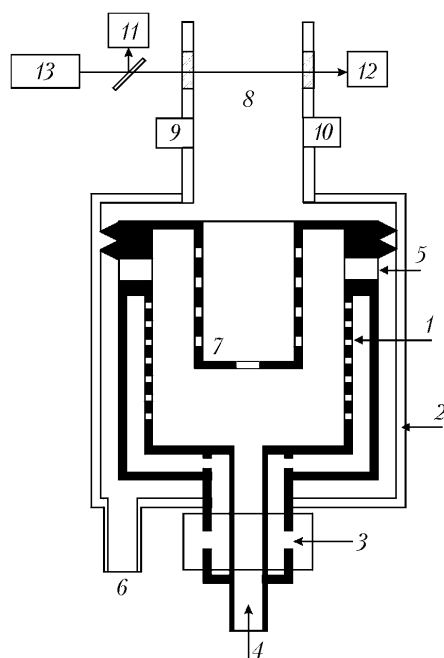


Fig. 1. Centrifugal bubble singlet-oxygen generator (the rotating part of the CBSOG is shown in black): 1) rotating bubbler; 2) shell; 3) channel for feeding bubbler; 4) channel for feeding the alkaline hydrogen peroxide solution; 5) holes for discharge of the alkaline hydrogen peroxide solution; 6) outlet pipe; 7) perforated cylinder; 8) chamber in which the parameters of the gas flow from the CBSOG are recorded; 9 and 10) germanium and silicon photodetectors; 11 and 12) photodetectors for the reference and probing beams of the nitrogen laser; 13) nitrogen laser.

ual chlorine, $O_2(^3\Sigma)$ and $O_2(^1\Sigma)$ oxygen, and steam. The content of $O_2(^1\Delta)$ in the region of its recording is determined by the quantum yield in reaction (1) and by the loss in the alkaline hydrogen peroxide solution and in the processes (3)–(5) in the gas path. In certain cases, e.g., to feed power to a chemical oxygen-iodine laser, it is desirable to have a high content of $O_2(^1\Delta)$ in relation to oxygen (more than 50%), a low content of the residual chlorine (less than 10%), and virtually the total absence of a dispersed liquid phase in the gas flow from the SOG. When the $O_2(^1\Delta)$ flow mixes with the vapor of molecular iodine, the latter dissociates into atoms; thereafter $O_2(^1\Delta)$ transfers energy to the iodine atoms $I(^2P_{3/2}) + O_2(^1\Delta) \leftrightarrow I(^2P_{1/2}) + O_2(^3\Sigma)$, causing the inverse population to form on the $^2P_{1/2} \rightarrow ^2P_{3/2}$ transition of an iodine atom in the oxygen-iodine laser [1].

The criteria of optimization of an SOG as a gas-liquid mass exchanger differ qualitatively from those for traditional chemical-technology apparatuses, since a high content of $O_2(^1\Delta)$ must be ensured in addition to the high degree of chlorine absorption. A few SOG types meeting these requirements have been created at present [1–4]. The first SOG for an oxygen-iodine laser was realized based on a bubble mass exchanger [1]. Under gravity conditions, the maximum specific load of bubble SOGs m_{Cl} is equal to 0.1 mmole/sec of chlorine per 1 cm² of the bubble layer at a total pressure above the solution layer of a few mm Hg [5]. Further increase in m_{Cl} is accompanied by the decline of chlorine utilization, a drop in the $O_2(^1\Delta)$ fraction, and a strong removal of the solution aerosol [5]. It is common knowledge that, when a bubble layer is in the field of large centrifugal accelerations (10^3 – 10^4 m/sec²), the diameter of the bubbles generated substantially diminishes, the velocity of their ascent grows, the mass-transfer rate multiply increases, and the spray removal decreases [6]. This is particularly favorable for $O_2(^1\Delta)$ gas generators designed for an oxygen-iodine laser where a high degree of chlorine utilization with simultaneous preservation of the high $O_2(^1\Delta)$ content must be ensured during the gas-liquid contact. In the present work, we give results of the first tests of a centrifugal bubble singlet-oxygen generator (CBSOG).

TABLE 1. Geometric Parameters of the CBSOGs Tested

CBSOG No.	S	a
1	7.5	6
2	1.33	6
3	6	3

Experimental Setup. A block diagram of the CBSOG is presented in Fig. 1. The CBSOG bubbler consists of a cylinder 1 with an inside diameter of 93 mm and a height of 100 mm, placed in shell 2. The revolution of the rotor is carried out with an electric motor. In the lateral cylinder wall, 550 cylindrical nozzles of length 9 mm and inside diameter 0.3 mm are arranged in a checkrow manner. The mixture of chlorine with helium was fed to the bubbler nozzles via channel 3. The alkaline hydrogen peroxide solution arrived at the interior surface of the rotating bubbler via channel 4 and was discharged into the receiving tank via a system of holes 5 and an outlet pipe 6. The bubble layer could be observed and photographed through a transparent upper cover. In bubbling, chlorine was absorbed by the solution and oxygen was formed in the process described in Eq. (1). The gas escaping from the bubble layer arrived at chamber 8, passing through a perforated cylinder 7. The gas temperature and the concentration of the residual chlorine and the steam were determined in the chamber and oxygen in the $O_2(^1\Delta)$ and $O_2(^1\Sigma)$ states was recorded. The total volume of the gas path from the bubbler surface to the measuring chamber was $\sim 480 \text{ cm}^3$. The pressure above the bubble layer was controlled by the cross section of holes in the rotating perforated cylinder 7, which was also a separator of coarse aerosol. The geometric parameters of the tested CBSOGs are presented in Table 1. The bubble-layer height for each CBSOG was controlled by changing the flow rate of the solution. The gas in the system was set flowing using an NV3-180 forepump.

The measuring chamber represented a short part of the gas channel of width 50 mm and height 15 mm. The concentration of the residual chlorine was determined from the attenuation of the probe beam of an N_2 laser (wavelength 337 nm). The spontaneous emissions of $O_2(^1\Delta)$ at a wavelength of 1278 nm and $O_2(^1\Sigma)$ at a wavelength of 762 nm were recorded respectively by germanium and silicon photodetectors equipped with optical filters. According to the balance of reactions (3) and (4), the concentration of $O_2(^1\Sigma)$ is in proportion to the concentration of $O_2(^1\Delta)$ squared and is in inverse proportion to the concentration of steam; consequently, $N_w = KI_{Ge}^2/I_{Si}$. Calibration of measurements of the residual concentration of chlorine N_{Cl} was reduced to measuring the cross section of absorption of emission at a wavelength of 337 nm by it. The measured cross section of chlorine absorption at this wavelength turned out to be equal to $(2.32 \pm 0.01) \cdot 10^{-19} \text{ cm}^2$, which was close to the value obtained in [7]. The coefficient K was determined earlier in investigating a jet SOG [8] where the same measuring chamber was used. Determination of the coefficient K was reduced to determination of the I_{Ge}^2/I_{Si} ratio, when the concentration of steam was known. The gas temperature in the measurement zone was determined by a thermocouple given a thin lubricating silicone coat to diminish the deactivation of $O_2(^1\Delta)$ on its surface. Data on the flow rates of helium and chlorine and on the pressure and temperature in the measuring chamber were sufficient for determining the partial pressures of helium, steam P_w , oxygen P_O , and the residual chlorine P_{Cl} , from which we computed the chlorine utilization $U = 1 - P_{Cl}/(P_{Cl} + P_O)$ and the relative content of steam $C_w = P_w/(P_{Cl} + P_O)$. The relative content of $O_2(^1\Delta)$ Y , which was in proportion to the I_{Ge}/P_O ratio, was evaluated by the lasing efficiency of the oxygen-iodine laser.

Experimental Results. The basic parameters varied in CBSOG tests were the height of the bubble layer, the arrangement of gas nozzles, the flow rates of the solution and chlorine, the rotational velocity of the bubbler, and the concentration composition of the alkaline hydrogen peroxide solution and its temperature. The alkaline hydrogen peroxide solution was prepared from a 14 M aqueous solution of KOH and 38% hydrogen peroxide in the corresponding proportions. The order in which the components were introduced into the CBSOG was as follows. Once the bubbler has been set in rotation, a mixture of helium with chlorine was fed to it; thereafter, nearly within 1 sec, the alkaline hydrogen peroxide solution was fed to the bubbler surface. As the bubble-layer height grew, the concentration of the residual chlorine dropped and the signals of the germanium and silicon photodetectors grew (Fig. 2). The bubble layer was photographed within 4 sec after the activation of the CBSOG, when the values of the bubble-layer thickness and of the parameters measured reached the steady state.

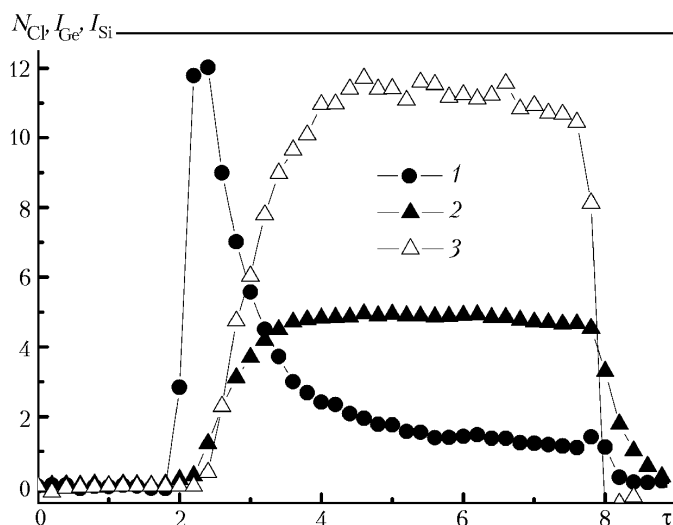


Fig. 2. Time dependence of the concentration of chlorine (1) and of the signals from the silicon (2) and germanium (3) photodetectors.

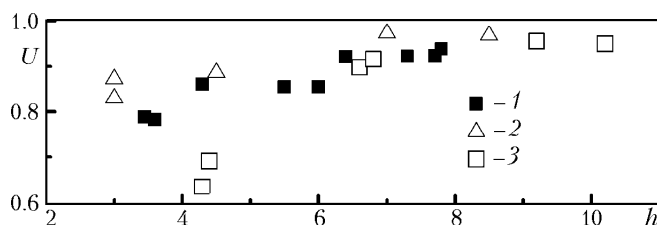


Fig. 3. Chlorine utilization vs. bubble-layer height ($n = 27 \text{ sec}^{-1}$, $M_{\text{Cl}} = 37 \text{ mmole/sec}$, and $M_{\text{He}} = 95 \text{ mmole/sec}$): 1) CBSOG-1, $N_{\text{H}} = 7.5 \text{ mole/liter}$, $N_{\text{b}} = 6 \text{ mole/liter}$, and $t = -20^{\circ}\text{C}$; 2) CBSOG-2, $N_{\text{H}} = 7.5 \text{ mole/liter}$, $N_{\text{b}} = 6 \text{ mole/liter}$, and $t = -20^{\circ}\text{C}$; 3) CBSOG-2, $N_{\text{H}} = 11 \text{ mole/liter}$, $N_{\text{b}} = 2 \text{ mole/liter}$, and $t = -15^{\circ}\text{C}$.

During the tests of CBSOG-1 and CBSOG-2, the rotational velocity of the bubbler was $n = 27 \text{ sec}^{-1}$; for this velocity, the centrifugal acceleration at the bottom of the bubble layer was equal to $1.34 \cdot 10^3 \text{ m/sec}^2$. Figure 3 presents the dependence of the chlorine utilization on the bubble-layer height growing with solution flow rate. For example, $h = 8 \text{ mm}$ was attained for a flow rate of the alkaline hydrogen peroxide solution of $180 \text{ cm}^3/\text{sec}$. The change from 3 to 9 mm in h led to a growth from 415 to 440 mm Hg in the gas pressure in front of the bubbler nozzles for CBSOG-1. The total pressure above the solution surface in CBSOG-1 was 35 mm Hg, whereas the total pressure on the bubbler surface was equal to 150 mm Hg at $h = 9 \text{ mm}$. With such a pressure difference on the nozzles the escape of the gas on their exit section was nearly critical. It is noteworthy that more than 60% of chlorine was utilized for $h \sim 3 \text{ mm}$. When h values were low, the efficiency of chlorine utilization for $N_{\text{b}} = 2 \text{ mole/liter}$ was somewhat lower than that for $N_{\text{b}} = 6 \text{ mole/liter}$ but became comparable if $h \approx 10 \text{ mm}$. The relative content of steam dropped with growth in the layer height, and it was lower for CBSOG-2 (Fig. 4) having a smaller cross section S . The $I_{\text{Ge}}/P_{\text{O}}$ ratio proportional to Y was independent of the bubble-layer height for CBSOG-1 and CBSOG-2 (Fig. 5). To additionally check this statement we measured the dependence of the chemical efficiency of the oxygen-iodine laser fed with oxygen from CBSOG-1 on the bubble-layer height. A detailed description of the oxygen-iodine laser with CBSOG-1 has been given in [9, 10]. By its chemical efficiency we mean the ratio of the photons emitted by the laser to the number of chlorine molecules introduced into the SOG. In laser experiments, CBSOG-1 operated under conditions where the utilization of chlorine, the content of steam, and the $I_{\text{Ge}}/P_{\text{O}}$ ratio were measured (Figs. 3–5). The laser tests showed (Fig. 6) that the efficiency of the oxygen-iodine laser increased with bubble-layer height in proportion to the chlorine utilization (see Fig. 3). This is possible if the parameter Y changes with increase in h only slightly. A chemical effi-

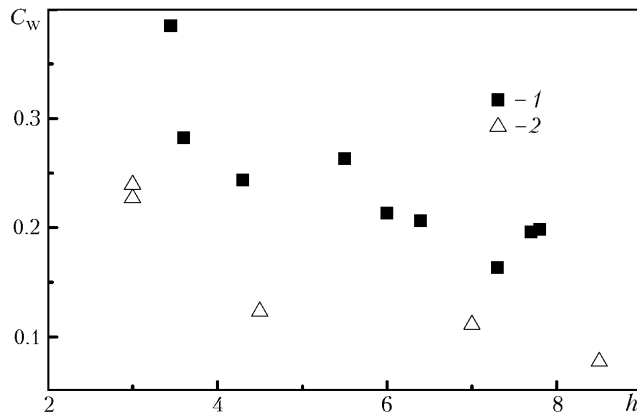


Fig. 4. Relative content of steam with change in the layer height ($n = 27 \text{ sec}^{-1}$, $M_{\text{Cl}} = 37 \text{ mmole/sec}$, $M_{\text{He}} = 95 \text{ mmole/sec}$, $N_{\text{H}} = 7.5 \text{ mole/liter}$, $N_{\text{b}} = 6 \text{ mole/liter}$, and $t = -20^{\circ}\text{C}$): 1) CBSOG-1; 2) CBSOG-2.

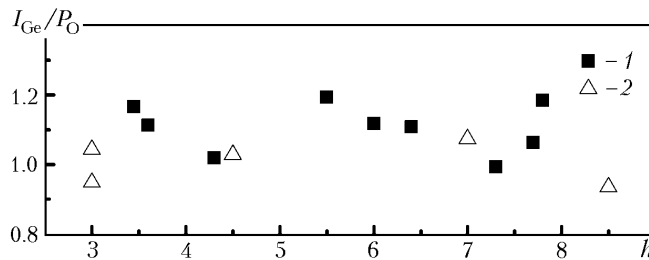


Fig. 5. Ratio $I_{\text{Ge}}/P_{\text{O}}$ vs. bubble-layer height ($n = 27 \text{ sec}^{-1}$, $M_{\text{Cl}} = 37 \text{ mmole/sec}$, $M_{\text{He}} = 95 \text{ mmole/sec}$, $N_{\text{H}} = 7.5 \text{ mole/liter}$, $N_{\text{b}} = 6 \text{ mole/liter}$, and $t = -20^{\circ}\text{C}$): 1) CBSOG-1; 2) CBSOG-2.

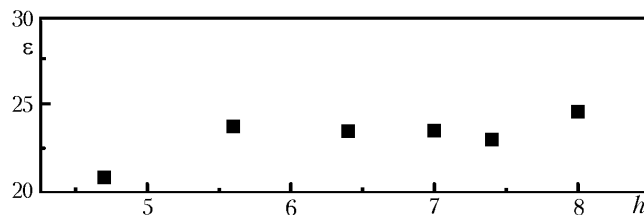


Fig. 6. Chemical efficiency of the oxygen-iodine laser vs. height of the bubble layer.

ciency of 25% of the oxygen-iodine laser in analogous small-scale units is attained when the relative content of $\text{O}_2(^1\Delta)$ is more than 50% [11, 12].

The rate of chlorine absorption during the chemical reaction (1) is determined not only by the concentration N_{b} but also by the diffusion of the reacting components in the solution. Reduction in the concentration N_{b} with simultaneous increase in the temperature of the alkaline hydrogen peroxide solution must lead to a growth in the mobility of the components in the solution. The concentration N_{b} was reduced by successive addition of distilled water to the initial solution with $N_{\text{H}} = 7.5 \text{ mole/liter}$ and $N_{\text{b}} = 6 \text{ mole/liter}$. The alkaline hydrogen peroxide solutions with lower values of N_{b} and N_{H} were prepared at elevated initial temperature to avoid ice formation. As is clear from Fig. 7, the chlorine utilization virtually remains constant with a decrease from 6 to 2 mole/liter in N_{b} , if the temperature of the solution is simultaneously increased. In these tests, the $I_{\text{Ge}}/P_{\text{O}}$ ratio was independent of the composition of the alkaline hydrogen peroxide solution and had the same scale as that in Fig. 5. The relative content of steam grew from 7 to 28% with a change from -21 and -5.3°C in the initial temperature of the alkaline hydrogen peroxide solution; this was not strange, since the pressure of the saturated steam above the bubble layer increased.

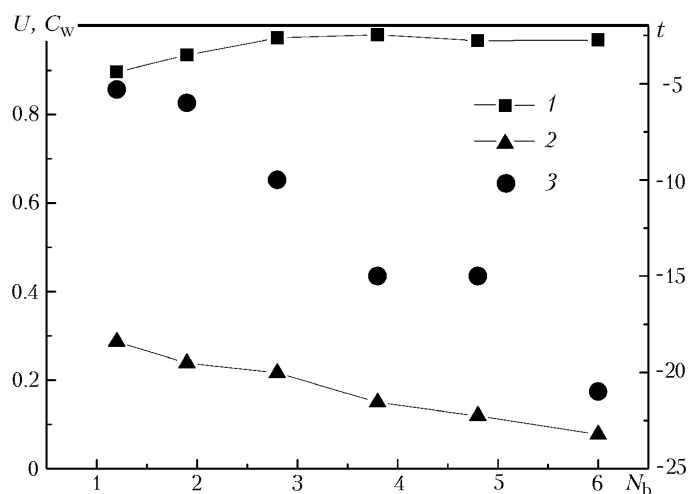


Fig. 7. Utilization of chlorine (1) and content of steam (2) vs. concentration of alkali. On the right-hand ordinate axis, the initial temperature of the solution (3) (CBSOG-2, $n = 27 \text{ sec}^{-1}$, $h = 7\text{--}8 \text{ mm}$, $M_{\text{Cl}} = 37 \text{ mmole/sec}$, and $M_{\text{He}} = 95 \text{ mmole/sec}$).

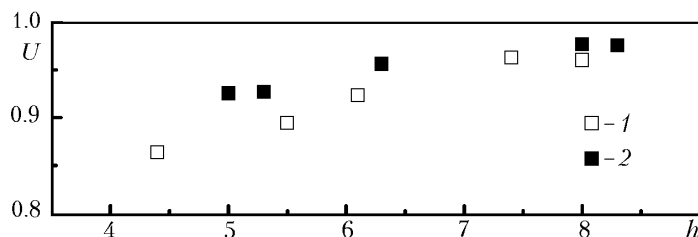


Fig. 8. Chlorine utilization vs. bubble-layer height for CBSOG-3 ($n = 46 \text{ sec}^{-1}$, $N_{\text{H}} = 7.5 \text{ mole/liter}$, $N_{\text{b}} = 6 \text{ mole/liter}$, and $M_{\text{He}} = 95 \text{ mmole/sec}$): 1) $M_{\text{Cl}} = 37$ and 2) 56 mmole/sec .

In testing CBSOG-3 with a closer packing of feed nozzles, the rotational velocity of the bubbler was increased to 46 sec^{-1} , for which the centrifugal acceleration on the bubbler surface was $3.88 \cdot 10^3 \text{ m/sec}^2$. The efficiency of chlorine utilization for the closer packing of the nozzles and higher rotational velocity of the bubbler is presented in Fig. 8. It is seen that the increase in the rotational velocity has led to a growth in the chlorine utilization for the same height of the bubble layer even for the higher flow rate of chlorine and the closer packing of the nozzles than those in CBSOG-1 and CBSOG-2. Also, it is noteworthy that the chlorine utilization was virtually the same for $M_{\text{Cl}} = 37$ and 56 mmole/sec . The value of the $I_{\text{Ge}}/P_{\text{O}}$ ratio was also independent of h in these tests and was coincident for $M_{\text{Cl}} = 37$ and 56 mmole/sec . The chemical efficiency of the oxygen-iodine laser operated with CBSOG-3 for $M_{\text{Cl}} = 56 \text{ mmole/sec}$ amounted to $\sim 25\%$ [9]. For the flow rates $M_{\text{Cl}} = 56 \text{ mmole/sec}$ and $M_{\text{He}} = 95 \text{ mmole/sec}$, the pressure above the bubble layer in CBSOG-3 was equal to 50 mm Hg . A unit load of total gas flow rate of $3 \text{ mmole/cm}^2/\text{sec}$ and a chlorine rate $m_{\text{Cl}} = 1.13 \text{ mmole/cm}^2/\text{sec}$ and a reduced velocity of the gas at the exit from the bubble layer of 11 m/sec were attained in this regime.

Discussion of Results. From the correlations obtained in [13, 14] for centrifugal bubble apparatuses, it follows that in the bubbling of a $\text{Cl}_2:\text{He}$ mixture of composition $\sim 1:2$ through an alkaline hydrogen-peroxide-solution layer of height $\sim 10 \text{ mm}$, bubbles with $r \approx 2 \text{ mm}$ and $V \approx 2.6 \text{ m/sec}$ for $n = 27 \text{ sec}^{-1}$ (CBSOG-1 and CBSOG-2) and with $r \approx 1.2 \text{ mm}$ and $V \approx 3 \text{ m/sec}$ for $n = 46 \text{ sec}^{-1}$ (CBSOG-3) are formed. Thus, if we have a bubble regime of bubbling, much of the chlorine (more than 60%) is absorbed for h comparable to the bubble diameter in the tests carried out. However, it must not be ruled out that a jet regime of bubbling rather than a bubble one is possible even under the conditions of high centrifugal acceleration for small bubble-layer heights and a sonic velocity of gas outflow from the nozzles. In any case such a degree of chlorine utilization for small h points to the high rate of mass transfer on the

initial portion of dispersion of the gas into the layer of the alkaline hydrogen peroxide solution. A weak dependence of the efficiency of chlorine absorption on the concentration of the alkali in the alkaline hydrogen peroxide solution enables us to assume that chlorine is absorbed in the regime of the reaction of pseudofirst order and of rapid hydrodynamic renewal of the reaction surface, and the resistance to mass transfer in the gas phase is insignificant. The CBSOG tests carried out and measurements of the efficiency of the oxygen-iodine laser have shown that the content of $O_2(^1\Delta)$ is weakly dependent on h within 4–10 mm. The time of residence of the gas in the bubble layer is, apparently, so short that the processes (3)–(5) occurring in it have no time to substantially reduce its concentration. For lower N_b values, the chlorine molecules must penetrate more deeply into the solution; the formation of $O_2(^1\Delta)$ in the process (1) must occur at larger distances from the liquid surface, and the time of its passage into the gas phase must be longer. The fact that the I_{Ge}/P_O ratio is independent of N_b that shows the change in the time residence of $O_2(^1\Delta)$ in the solution is much smaller than its lifetime in it of $2 \cdot 10^{-6}$ sec. The efficiency (25%) of the chemical oxygen-iodine laser fed by oxygen from the CBSOG has turned out to be a quantity comparable to the efficiency obtained in other works in which the fraction of singlet oxygen is $Y > 50\%$ [11, 12]. From this comparison it may be inferred that the CBSOG generates oxygen in which more than 50% of it is in the $O_2(^1\Delta)$ state. Since no aerosol was visually observed at the CBSOG outlet, we may assume that all large droplets removed by the gas from the bubble layer return to it again or arrive at the rotating perforated cylinder. The droplets deposited on the perforated cylinder may be thrown into the bubble layer again or be capable of serving as a source of ultradisperse aerosol removed by the gas flow. The growth in the partial pressure of steam due to the evaporating ultradisperse aerosol is determined by its volume fraction in the gas flow. A strong dependence of the content of steam in the measuring chamber on the initial temperature of the alkaline hydrogen peroxide solution (Fig. 7) suggests that the contribution due to the vaporization inside the bubble layer is substantially higher than that due to the volume fraction of the aerosol. This is also supported by the higher relative content of steam in the case of larger S where the partial pressure of oxygen together with the residual chlorine above the bubble layer is lower.

Conclusions. In the range of the CBSOG regimes investigated, a more than 90% utilization of chlorine occurs for a bubble-layer thickness of 6–10 mm. The content of $O_2(^1\Delta)$ is weakly dependent on the height of the bubble layer and the composition of the alkaline hydrogen peroxide solution. The high chemical efficiency of the oxygen-iodine laser fed by oxygen from the CBSOG enables us to assume that the relative fraction of $O_2(^1\Delta)$ at its outlet exceeds 50%. In the tests carried out, no removal of the droplets of the alkaline hydrogen peroxide solution is visually observed. The content of steam in the gas flow at the CBSOG outlet is mainly determined by the process of evaporation inside the bubble layer, i.e., by its certain average temperature. Compaction of the feed nozzles with simultaneous increase in the centrifugal acceleration enables us to raise the unit chlorine load to $1.13 \text{ mmole/cm}^2/\text{sec}$ with preservation of the degree of chlorine utilization of more than 90% and a content of $O_2(^1\Delta)$ of higher than 50%. The specific oxygen output of more than $1 \text{ mmole/cm}^2/\text{sec}$ attained under the conditions of stable CBSOG operation without spray removal is one order of magnitude higher than the outlet of bubble SOGs [5] operating under gravity conditions. The high chemical efficiency of the CBSOG-based oxygen-iodine laser shows that it is a promising high-yield source of singlet oxygen.

This work was carried out with financial support from the European Office of Aerospace Research and Development EOARD (project 057003) and with administrative support from the International Scientific-Technical Center (grant No. 3380P) and the Russian Foundation for Basic Research (grant 05-08-014585a).

NOTATION

a , distance between the bubbler nozzles, mm; C_w , relative content of steam; h , bubble-layer height, mm; I_{Ge} , output signal of the germanium photodetector, rel. units; I_{Si} , output signal of the silicon photodetector, rel. units; K , calibration factor; M_{Cl} , flow rate of chlorine, mmole/sec; M_{He} , flow rate of helium, mmole/sec; m_{Cl} , flow rate of chlorine per 1 cm^2 of the bubbler, mmole/cm²/sec; n , rotational velocity of the bubbler, sec⁻¹; N_H , concentration of hydrogen peroxide in the alkaline hydrogen peroxide solution, mole/liter; N_b , concentration of alkali in the alkaline hydrogen peroxide solution, mole/liter; N_{Cl} , concentration of chlorine in chamber 8, mole/cm³; N_w , concentration of steam in chamber 8, mole/cm³; P_O , P_{Cl} , and P_w , partial pressures of oxygen, chlorine, and steam in chamber 8, mm Hg; r , bubble radius, mm; S , cross-sectional area of holes for passage of the gas in the perforated cylinder, cm²; t , initial

temperature of the alkaline hydrogen peroxide solution, °C; V , velocity of ascent of a bubble, m/sec; U , chlorine utilization; $Y = [\text{O}_2(^1\Delta)]/([\text{O}_2(^1\Delta)] + [\text{O}_2(^3\Sigma)])$, relative content of $\text{O}_2(^1\Delta)$; Y_{los} , loss of the relative content of $\text{O}_2(^1\Delta)$ in the resonator of the oxygen-iodine laser by dissociation of molecular iodine, quenching, and removal of the threshold fraction from the resonator; $\varepsilon = 100U\eta(Y - Y_{\text{los}})$, chemical efficiency of the oxygen-iodine laser, %; η , optical efficiency of the resonator of the oxygen-iodine laser; τ , running time from the beginning of the startup of the CBSOG, sec. Subscripts: b, alkali; w, water; los, loss.

REFERENCES

1. W. E. McDermott, N. R. Pchelkin, D. J. Benard, and R. R. Bousek, An electronic transition chemical laser, *Appl. Phys. Lett.*, **32**, No. 8, 469–470 (1978).
2. M. V. Zagidullin, A. Yu. Kurov, N. L. Kupriyanov, V. D. Nikolaev, M. I. Svistun, and N. V. Erasov, A high-efficiency jet $\text{O}_2(^1\Delta)$ generator, *Kvantovaya Elektron.*, **18**, No. 7, 826–832 (1991).
3. K. R. Kendrick, C. A. Helms, and B. G. Quillen, Determination of singlet-oxygen generator efficiency on a 10-kW class supersonic chemical oxygen-iodine laser (RADICL), *IEEE J. Quant. Electron.*, **35**, No. 12, 1759–1763 (1999).
4. J. A. Blauer, S. A. Munjee, K. A. Truesdell, E. C. Curtis, and J. F. Sullivan, Aerosol generators for singlet oxygen production, *J. Appl. Phys.*, **62**, No. 6, 2508–2516 (1987).
5. V. N. Azyazov, N. P. Vagin, N. L. Kupriyanov, and N. N. Yuryshv, Experimental and theoretical investigation of a singlet oxygen bubbler generator for an oxygen-iodine laser, *J. Soviet Laser Res.*, **14**, 114–126 (1993).
6. A. I. Safonov and V. S. Krylov, Laws governing heat- and mass transfer in rotating bubbling beds, in: *Proc. 5th All-Union Heat- and Mass Transfer Conf.*, [in Russian], Vol. 4, Minsk (1976), pp. 85–93.
7. S. Hubinger and J. B. Hee, Absorption spectra of Cl_2 , Br_2Br_2 , and BrCl between 190 and 600 nm, *J. Photochem. Photobiol. A, Chemistry*, **86**, 1–7 (1995).
8. M. V. Zagidullin, V. D. Nikolaev, M. I. Svistun, and N. A. Khvatov, Efficient COIL driven by SOG with filament-guided jets, *Proc. SPIE*, **5777**, 58–61 (2005).
9. M. V. Zagidullin, V. D. Nikolaev, M. I. Svistun, and N. A. Khvatov, An ejector oxygen-iodide laser with a centrifugal bubble singlet-oxygen generator, *Kvantovaya Elektron.*, **35**, No. 10, 907–908 (2005).
10. M. V. Zagidullin, V. D. Nikolaev, M. T. Svistun, and G. D. Hager, Efficient chemical oxygen-iodine laser powered by a centrifugal bubble singlet oxygen generator, *Appl. Phys. Lett.*, **86**, No. 23, 25–26 (2005).
11. M. Endo, S. Nagatomo, S. Takeda, M. V. Zagidullin, V. D. Nikolaev, H. Fujii, F. Wani, D. Sugitomo, D. Sunako, K. Nanri, and T. Fujioka, High-efficiency operation of chemical oxygen-iodine laser using nitrogen as buffer gas, *IEEE J. Quant. Electron.*, **34**, No. 3, 393–398 (1998).
12. T. L. Rittenhouse, S. P. Phipps, and C. A. Helms, Performance of a high-efficiency 5-cm gain length supersonic chemical oxygen-iodine laser, *IEEE J. Quant. Electron.*, **35**, No. 6, 857–866 (1998).
13. A. I. Safonov, V. S. Krylov, and P. A. Gorshenin, Laws governing gas dispersion into a rotating layer of liquid, *Teor. Osnovy Khim. Tekhnol.*, **7**, No. 3, 448–451 (1973).
14. A. I. Safonov and V. S. Krylov, Motion of a single bubble in a rotating layer of liquid, *Teor. Osnovy Khim. Tekhnol.*, **7**, No. 2, 267–269 (1973).